A Study of Isotherms and Kinetics of Mangifera Indica Bark Adsorbent Used for Fluoride Removal form Drinking Water

Abhishek Kumar
Department of Civil Engineering
National Institute of Technology Patna
Patna, India
abhishek.ce18@nitp.ac.in

Nityanand Singh Maurya
Department of Civil Engineering
National Institute of Technology Patna
Patna, India
nsmaurya@nitp.ac.in

Received: 14 July 2022 | Revised: 26 July 2022 | Accepted: 2 August 2022

Abstract-In this paper, we have investigated the bark of mango (Mangifera Indica) as an adsorbent for fluoride removal. Chemical treatment and aluminum hydroxide coating increased the adsorption capacity of the adsorbent from 0 to 15mg/g. Aluminum hydroxide-coated adsorbent (Al-MIBAC) was subjected to a batch study by considering different operational parameters such as adsorbent dose, reaction time, and pH. The kinetics of the adsorbent strongly followed second-order behavior, indicating the chemo-sorption adsorption process. The R2 value for Langmuir isotherm is 0.999 and it was found to be fitted well with the experimental data. It is hence assumed that the adsorption of fluoride is homogeneous and monolayer. The maximum fluoride adsorption amount of Al-MIBAC was 56.81mg/g, which was superior to those of other adsorbents derived from bark. Al-MIBAC was highly effective in reducing the fluoride concentration from 20mg/L to less or equal to 1.5mg/L which is safe for drinking purposes.

Keywords-adsorption; Al-MIBAC; activated carbon; fluoride removal; isotherm; kinetics; mangifera indica

I. INTRODUCTION

Fluoride is a well-known pollutant present in drinking water. As per WHO, the allowable limit of fluoride concentration in drinking water is 1.5mg/L, whereas BIS, recommended 1mg/L [1]. Fluoride is beneficial for the bones and teeth if present in acceptable limits, otherwise it may cause dental and skeletal fluorosis, brittle bones, thyroid disorder, Alzheimer's syndrome, arthritis, brain damage, infertility, cancer, osteoporosis, and damage DNA structure [2, 3]. Natural process such as weathering and leaching of fluoride rich minerals, and anthropogenic processes like industrial discharging, biomass burning, mining, and extensive use of fertilizers are major sources of fluoride contamination in groundwater [4]. Authors in [5] reported the appearance of excessive fluoride concentration in drinking water in more than 25 countries. Approximately 200 million people around the world are facing serious problems of very high fluoride exposure through drinking water [5]. Therefore, there is a high priority to deal with this problem, to ensure safe drinking water [6]. For this purpose, several methods such as precipitation, electro-coagulation, ion-exchange, membrane technology, and adsorption have been used to remove such pollutants [7]. Each of them has some benefits and drawbacks [8]. Precipitation/coagulation and electrocoagulation produce huge amounts of sludge. In ion-exchange process, the high operational cost is a major drawback. Membrane process has high initial and maintenance cost coupled with wasting huge amounts of water. Frequent fouling or scaling results in reduced useful life of membrane filters [7]. Among all the removal methods, adsorption is eco-friendly, with low cost, is less tedious in operation, and possesses high removal capacity [9]. Several studies have been conducted on various types of adsorbents, such as biological materials (bio-adsorbents), metal hydroxides and oxides, geomaterials, industrial by-products, etc. The best outcome and greatest adsorption capability among the adsorbents mentioned above are demonstrated by carbonaceous materials, particularly those loaded with oxides and hydroxides of metals. Activated carbon derived from Indian mulberry (Morinda Tinctoria), Gular bark (Ficus racemosa), Babool bark (Acacia nilotica bark), and Mangifera indica bark have been previously used in the removal of fluoride from drinking water [10-12, 14]. To enhance the performance, activated carbon has also been treated with metal hydroxides and oxides, such as Al-impregnated eucalyptus bark ash, aluminum hydroxide coated Morinda Tinctoria bark, etc. [11, 13].

In the present study, a novel adsorbent is proposed and prepared using aluminum hydroxide coated activated carbon of mango (mangifera indica) bark for the effective removal of fluoride from drinking water. The parameters considered were pH, adsorbent dose, and reaction time. Three widely used kinetics and isotherm models were employed to the experimental data. This paper will investigate the mechanism of adsorption followed between adsorbent's surface and fluoride ions. The developed adsorbent exhibits an adsorption capacity of 56.81mg/g which is significantly higher in comparison to many other materials as presented in Table I.

Corresponding author: Nityanand Singh Maurya

TABLE I. ADSORPTION CAPACITY OF DIFFERENT PLANT BARKS

Adsorbent	Reaction Time	Dose (g/L)	Adsorption capacity (mg/g)	Ref.
AC acacia nilotica bark	8 h	5	1.891	[10]
AC morinda tinctoria	60 min	0.1	26.028	[11]
Al- impregnated eucalyptus bark ash	30 min	0.1	3.922	[13]
AC ficus- racemosa plant	60 min	4	1.549	[12]
AC mangifera bark	90 min	2	1.862	[14]
Al $(OH)_3$ coated mango bark	24 h	0.3	56.81	Present work

II. MATERIALS AND METHODS

A. Plant Description

There is a variety of plant barks indicated in the literature and tested against the adsorption of fluoride present in surface or ground water. In the present study, Mangifera Indica (mango) Bark (MIB) was used to prepare the adsorbent. Mangifera indica, an evergreen tree of anacardiaceae family is commonly found in tropical regions like India. It grows to a hight of 10-45 m, dome shaped with dense foliage, typically heavy branched from a stout trunk. Different parts of mangifera indica have different pharmacological and therapeutic properties: the juice of unripe mango fruit is used in heat strokes, the seeds are used in asthma and astringent treatment, fumes of burning leaves are used for hiccups, and the bark is used in the treatment of menorrhagia, anaemia, scabies, cutaneous infections, syphilis, diabetes, diarrhoea, etc. [15, 16].

B. Bark Collection

The bark was carefully removed from the stem, without disturbing its inner parts, from the top (25 cm below the lowest branch) to the bottom (25 cm above the highest root). The cut width was not larger than 20 cm, thus the environmental impact of mango stem bark collection was minimal.

C. Chemicals

Analytical grade chemicals were used in the present study. Sodium fluoride (NaF), aluminum sulphate $(Al_2(SO4)_3.16H_2O)$, sodium hydroxide (NaOH), and hydrochloric acid (HCl) were obtained from the local market. Test solutions were prepared using distilled water.

D. Preparation of the Activated Carbon

After collection, the MIB was cut into small pieces and dried in hot air oven at 65°C to remove moisture. The dried bark was powdered using a kitchen grinder. To obtain the desired particle size bark powder, the grinded bark was sieved using a 425 µm mesh size. For removal of dust and color, it was shocked in diluted nitric acid solution for 24 hours with occasional mixing and was washed several times with distilled water until the wash water pH approached neutral value. The washed MBI powder was dried in hot air oven. To obtain activated carbon from the MBI, it was placed in muffle furnace under anoxic condition at 450°C for 1 hour with uniform increase in temperature of 2°C/min.

E. Coating of Aluminium Hydroxide on Activated Carbon

Firstly 600 mL, 0.6M aluminum sulphate solution were poured into the beaker, followed by the slow addition of 100 gm ready MIBAC to the beaker as shown in [17]. Proper mixing was done to ensure complete mixing of MIBAC into the aluminum sulphate solution. Afterwards, 3M of sodium hydroxide were slowly added into the mixture. Sodium hydroxide reacts with aluminum sulphate and precipitates of aluminium hydroxide were formed. The precipitates were deposited on the MIBAC surface. The pH of the reaction mixture controls the addition of sodium hydroxide, which stopped once the pH reached the target range of 5-7. The resultant mixture contains aluminum hydroxide coated MIBAC and sodium salt. This slurry was filtered with vacuum pressure filter. The filtered materials were dried at 110 °C to complete the coating of aluminum hydroxide. To eliminate the sodium sulphate salt before conducting further tests, the Al-coated MIBAC was thoroughly rinsed with distilled water. Washing continued until the output water contained less than 1 mg/L of sulphate ions. The washed MIBAC was dried at 65 °C for 12 hours and was stored in an air tight bottle for adsorption experiments [17].

III. EXPERIMENTAL PROCEDURE

A. Fluoride Stock and Test Solution Preparation

An amount of 2.21g sodium fluoride were dissolved in 1 L distilled water, to make a stock solution of 100 mg/L concentration stored in 1 L reagent bottle. To prepare the test solution the fluoride stock solution was diluted 5 times to achieve 20 mg/L concentration.

B. Adsorption Experiment

Batch adsorption equilibrium isothermal study was conducted by adding an appropriate dose of adsorbent in 200 ml reagent bottles containing 100 ml fluoride solution of 20 mg/L concentration. The bottles were loaded on an orbital shaker at 100 revolution per minutes at 25 ± 2 °C. By ensuring adequate reaction time, the resultant mixture was separated using 0.45 µm Whatman's filter paper and the filtrate was collected for residual fluoride. Kinetics experiment was performed in a cylindrical vessel of 2 L capacity. A speed-controlled mixer was used to mix the solution at the desired mixing speed. The experiment was conducted at adsorbent dose of 0.3 g/L, initial concentration 20 mg/L, and initial pH 6.5. The cylindrical vessel was partially submerged in water bath to maintain a constant temperature of 30 ± 2 °C. To study the effect of the initial pH on the removal percentage, the pH was adjusted from 2.35 to 10.25 using 0.1M NaOH and 0.1M HCl solutions. To determine the effect of adsorbent dose on fluoride removal and adsorption capacity, 100 ml of fluoride solution having 20 mg/L concentration reacted with different adsorbent doses of 100, 300, 600, 900, and 1200 mg/L. The experiments were performed in triplicates. The fluoride adsorption capacity was calculated as:

$$q_e = \frac{(C_i - C_e) \times V}{W} \quad (1)$$

where Ci and Ce are the initial and equilibrium concentrations of test solution, q_e is the equilibrium adsorption capacity

(mg/g), W is the mass of the absorbent (mg), and V the volume of test solution (ml) [18].

The percentage removal was calculated from (2):

$$\% \text{ Removal } = \frac{Ci-Ce}{Ci} \times 100 \quad (2)$$

IV. RESULTS AND DISCUSSION

A. Batch Adsorption Studies

1) Effect of pH on the Removal of Fluoride

In order to investigate the effect of initial pH on fluoride removal from drinking water, the initial pH of the fluoride solution varied pH from 2.35 to 8.49 using 0.1M NaOH and 0.1M HCl solutions. The initial concentration of fluoride and the adsorbent dose were kept similar at all pH values. Figure 1 indicates that fluoride removal efficiency is a function of pH and maximum fluoride removal took place at pH=5.35. Authors in [19] observed maximum removal efficiency at pH=7 during the adsorption of fluoride on aluminum hydroxide-coated activated carbon of morinda tinctoria. Authors in [8] also reported maximum adsorption at pH=6 for a composite adsorbent prepared activated carbon of egg cell and rice straw. At lower pH values, removal efficiency decreases due to the formation of weak hydrofluoric acid and complexations of fluoride ions with aluminium [19]. After pH=5.35, continuous decrease in fluoride removal was observed. The main reason behind this decrease is the repulsive force between the hydroxide and fluoride ions available on the adsorbent surface and aqueous solution. It was also reduced due to the competition of hydroxide and fluoride ions to bind on the surface of Al-MIBAC [20].

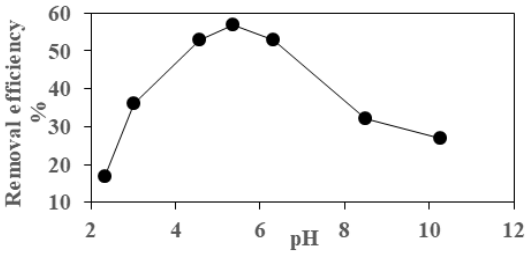

Fig. 1. Effect of pH.

2) Effect of the Adsorbent Dose on Fluoride Removal

To investigate the impact of adsorbent dose on fluoride removal from polluted drinking water, varying adsorbent doses of 0.3 g/L to 1.2 g/L, at pH 6.5, and temperature 25 ± 2 °C were mixed with 20 mg/L initial fluoride concentration. From Figure 2, it is observed that removal efficiency increases drastically from 21 to 86.5%, when the dose of the adsorbent increased from 0.1g/L to 0.9 g/L. Further increase of the dose up to 1.2 g/L results to gradual increase to 90%. The rise in removal efficiency with increasing adsorbent dose is caused by the increase of the presence of active sites. However, with increase in adsorbent dose, the amount of fluoride absorbed per unit weight of the adsorbent decreased. This decrease may be caused by the increase of adsorbent-adsorbent contact instead of fluoride contact with adsorbent surface. As a result, adsorbent-adsorbent contact causes the adsorbent particles to aggregate [21]. Because of this overlap, there are fewer active sites on the adsorbent particles' surface, which inhibits the surface area from growing as a result of increased adsorbent dosages. Authors in [22] reported similar results during the adsorption of fluoride on potent nanocrystalline hydroxyapatite surface.

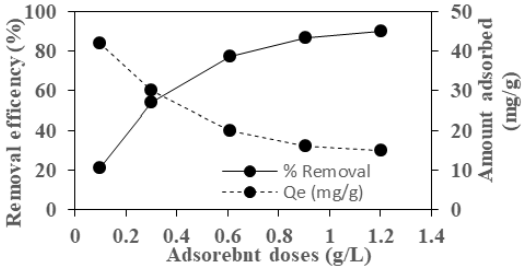

Fig. 2. Dose effect.

B. Batch Adsorption Equilibrium Isotherm

Fluoride removal capacity was investigated by varying the dose of adsorbent from 0.3 g/L to 1.2 g/L at 20 mg/L initial fluoride concentration, initial pH 6.5, contact time 24 hours, and 25 ± 2 °C temperature. Three commonly used isotherm models namely Langmuir, Freundlich and Temkin isotherm models were employed to fit the experimental data. The related parameters are presented in Table II.

TABLE II. OBTAINED ISOTHERM PARAMETERS

Isotherm	Parameters	Value
Langmuir	K_L	0.182
	Q_m	56.81
	R^2	0.9991
Freundlich	K_f	11.3516
	n	2.0157
	R^2	0.9812
Temkin	A_T	1.5478
	B	13.249
	R^2	0.9975

1) Langmuir Isotherm Model (LIM)

LIM considers a specific number of active adsorption sites present on the surface of the adsorbent. Only one adsorbate molecule can be absorbed by each active site. The adsorption process may be considered completed if all the active sites are occupied by the adsorbate. This adsorption is monolayer in nature with constant adsorption energy [23]. The linear from of LIM is expressed as:

$$\frac{C_e}{q_e} = \frac{1}{K_l q_m} + \frac{C_e}{q_m} \quad (3)$$

where q_m is the maximum adsorption capacity, C_e is the equilibrium concentration, K_l is the Langmuir constant, q_m and K_l are calculated by plotting the graph between $\frac{C_e}{q_e}$ vs C_e (Figure 3). The values of q_m and K_l obtained from LIM are 56.81 and 0.182 respectively. The regression coefficient R^2 is 0.9991 indicating a very good fit. Authors in [8, 11] reported that aluminium impregnated composite adsorbent follows the Langmuir isotherm.

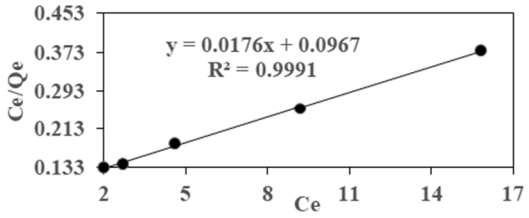

Fig. 3. Langmuir isotherm.

2) Freundlich Isotherm Model (FIM)

FIM is an empirical model applicable for multilayer adsorption process. It considers heterogeneous absorbent surface with varying affinity for adsorption. The experimental data were employed in FIM to obtained the value of Freundlich constants (n) and (K_F) [23]. This model is expressed as:

$$\ln q_e = \ln K_F + \frac{1}{n}\ln C_e \quad (4)$$

The graph between $\ln q_e$ and $\ln C_e$ is shown in Figure 4. The values of Freundlich constant and exponent were determined by slope and intercept respectively.

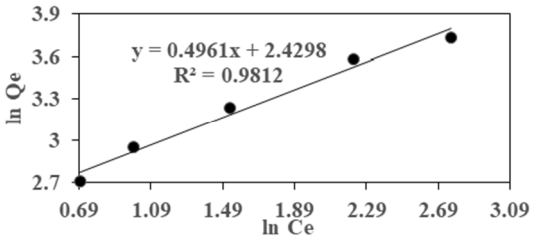

Fig. 4. Freundlich isotherm.

3) Temkin Isotherm Model (TIM)

TIM was proposed in 1940. This model describes that the heat of adsorption between adsorbate and adsorbent molecule decreases linearly due to the interactions between adsorbed molecules on the surface [24]. TIM model is expressed as:

$$q_e = \frac{RT}{b_T}\ln A_T + \frac{RT}{b} \quad (5)$$

$$q_e = B\ln A_T + B\ln C_e \quad (6)$$

where $B = \frac{RT}{b_T}$, b_T is the Temkin isotherm constant, A_T is the binding constant at equilibrium (L/g), B is a constant corresponding to the heat of sorption (J/mol), R is the universal gas constant (J/mol K), and T the temperature in Kelvin.

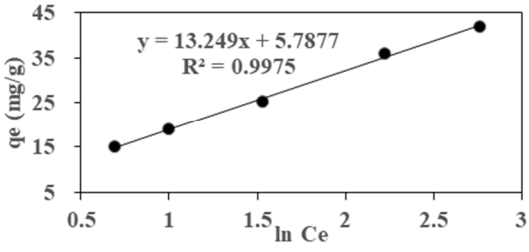

Fig. 5. Temkin isotherm.

The R^2 value of TIM is 0.997 and fitted well with the experimental data. To evaluate the B and A_T, a graph q_e vs $\ln C_e$ is plotted Figure 5. The obtained values of B and A_T from slope and intercept are 13.294 J/mol and 1.5478 L/g. Among the models applied to the experimental data in the present study, Langmuir was the better fitted model with R^2 = 0.9991 regression. Thus, LIM describes better the adsorption isotherm behavior as compared to TIM (R^2 = 0.9975) and FIM (R^2 = 0.9812).

C. Kinetics Study

Adsorption kinetics provides relations between reaction time and adsorption capacity (Figure 6). The effect of reaction time on fluoride adsorption was observed by changing reaction time from 5 min to 37 hours, with initial fluoride concentration of 20 mg/L, at pH=6.5 and temperature 30 ± 2°C. Kinetics also provides information about the mechanism of adsorption, the surface, and the nature of the adsorbent. The linear from of the three kinetics models, namely Pseudo First Order (PFO), Pseudo Second Order (PSO), and Intra-Particle Diffusion (IPD) model were employed on the experimental data.

1) Pseudo First Order

PFO is based on the assumption that the change in solute uptake rate over time is directly proportional to the difference in saturation concentration and quantity of the solid uptake with time. The linear from of PFO is:

$$\ln(q_e - q_t) = \ln q_e - K_1 t \quad (7)$$

where q_e and q_t are the adsorption capacity at equilibrium and at time t (mg/g), K_1 is the rate constant, and t is the reaction time. The plot $\ln(q_e - q_t)$ vs t, gives slope = -0.0015 and intercept = 2.3169 with a regression coefficient R^2 = 0.5675, indicating that PFO does not fit the observed data.

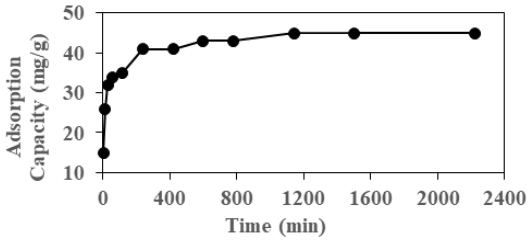

Fig. 6. Adsorption capacity.

2) Pseudo Second Order

It is based on the assumption that the rate-limiting step is chemical sorption or chemisorption and predicts the behavior over the whole range of adsorption. In this condition, the adsorption rate is dependent on the adsorption capacity, not on the concentration of the adsorbent. The main difference of PSO over PFO is that, in PSO equilibrium, the adsorption capacity is obtained from the model and does not need to be calculated theoretically form adsorption experiments [25]. The linear from of PSO is:

$$\frac{t}{q_t} = \frac{1}{K_2 q_e^2} + \frac{t}{q_e} \quad (8)$$

where K_2 is a seconded order rate constant (mg/g min).

The linear fit as per (8) is given in Figure 7, and indicates excellent fit with a very high regression coefficient R^2 = 0.9996. The adsorption capacity obtained from PSO kinetics is 45.24 mg/g and $K_2 = 1.063\times 10^{-3}$. The lower value of K_2 indicates that the rate of fluoride sorption is fast.

3) Intra-Particle Diffusion

The mass transfer diffusion model [26] is described by:

$$q_t = K_p t^{0.5} + C \quad (9)$$

where K_p is the intra-particle diffusion rate constant and C is a constant related to boundary layer thickness

If IPD controls the adsorption process, the q_t vs $t^{0.5}$ plot will be a straight line indicating IPF is a rate determining step. However, if nonlinearity is observed, it would indicate that several processes control the mechanism involved in rate limiting steps. From the plot in Figure 8 between q_t and $t^{0.5}$, it is observed that three steps control the adsorption process. Each step among the three is the rate limiting step at specific time intervals. The rate of adsorption calculated from the slope of linear portion, if the slope is increased at a sharp rate, the adsorption is faster. As a result, the beginning of the straight line with a step slop passing close to the origin indicates that the rate of initial diffusion through micropores and mesopores is high. The second straight portion of plots indicates fluoride diffusion through micropores and the last straight segments represents the modest adsorption on the adsorbent [8]. It is reported that pseudo second order are best fitted during adsorbent kinetics of fluoride on aluminum hydroxide coated activated carbon prepared from bark of morinda tinctoria [11]. Authors in [8] also reported that during the adsorption, second order kinetics nicely fit the kinetics of fluoride on aluminum impregnated composite adsorbent.

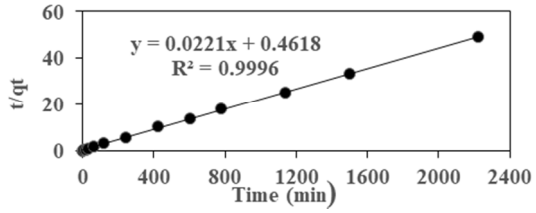

Fig. 7. Pseudo second order.

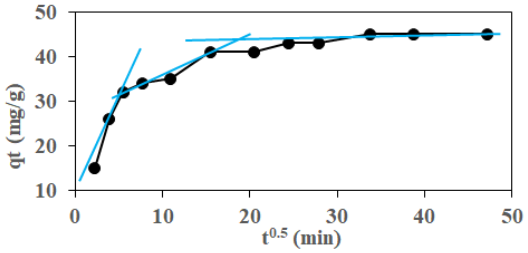

Fig. 8. Intra-particle diffusion model.

V. CONCLUSION

Mangifera indica, commonly known as mango, is a significant herb in the ayurvedic and traditional medicine. In this study, we used mangifera indica bark for fluoride removal from drinking water. Its fluoride adsorption efficiency was improved by chemical treatment. Aluminum hydroxide coated mangifera bark adsorbent was developed for fluoride removal. Aluminum coating on the activated Carbon of MIBAC not only increased the affinity towards fluoride, but also increased the adsorbent surface, thus improving its adsorption capacity. A batch study on Al-MIBAC was conducted by considering different operational parameters like dose, reaction time, and initial pH at constant temperature of 25 ± 2 °C. The best fitted kinetics of Al-MIBAC was the second order kinetics with R^2 = 0.9996. All analyzed models fitted good, but the Langmuir model exhibited the best fit with the experimental data with R^2 = 0.9991, which indicates monolayer and homogeneous adsorption. Temkin and Freundlich isotherms also assumed to contribute partially in the adsorption.

REFERENCES

[1] S. Ayoob and A. K. Gupta, "Fluoride in Drinking Water: A Review on the Status and Stress Effects," *Critical Reviews in Environmental Science and Technology*, vol. 36, no. 6, pp. 433–487, Dec. 2006, https://doi.org/10.1080/10643380600678112.

[2] A. Ghosh, K. Mukherjee, S. K. Ghosh, and B. Saha, "Sources and toxicity of fluoride in the environment," *Research on Chemical Intermediates*, vol. 39, no. 7, pp. 2881–2915, Sep. 2013, https://doi.org/10.1007/s11164-012-0841-1.

[3] A. N. Laghari, Z. A. Siyal, D. K. Bangwar, M. A. Soomro, G. D. Walasai, and F. A. Shaikh, "Groundwater Quality Analysis for Human Consumption: A Case Study of Sukkur City, Pakistan," *Engineering, Technology & Applied Science Research*, vol. 8, no. 1, pp. 2616–2620, Feb. 2018, https://doi.org/10.48084/etasr.1768.

[4] B. Karthikeyan and E. Lakshmanan, "Fluoride in Groundwater: Causes, Implications and Mitigation Measures," in *Fluoride Properties, Applications and Environmental Management*, S. D. Monroy, Ed. 2011, pp. 111–136.

[5] N. Adimalla, S. Venkatayogi, and S. V. G. Das, "Assessment of fluoride contamination and distribution: a case study from a rural part of Andhra Pradesh, India," *Applied Water Science*, vol. 9, no. 4, May 2019, Art. no. 94, https://doi.org/10.1007/s13201-019-0968-y.

[6] K. Praveen and L. B. Roy, "Assessment of Groundwater Quality Using Water Quality Indices: A Case Study of Paliganj Distributary, Bihar, India," *Engineering, Technology & Applied Science Research*, vol. 12, no. 1, pp. 8199–8203, Feb. 2022, https://doi.org/10.48084/etasr.4696.

[7] S. Ayoob, A. K. Gupta, and V. T. Bhat, "A Conceptual Overview on Sustainable Technologies for the Defluoridation of Drinking Water," *Critical Reviews in Environmental Science and Technology*, vol. 38, no. 6, pp. 401–470, Sep. 2008, https://doi.org/10.1080/10643380701413310.

[8] A. Saini, P. H. Maheshwari, S. S. Tripathy, S. Waseem, A. Gupta, and S. R. Dhakate, "A novel alum impregnated CaO/ carbon composite for de-fluoridation of water," *Groundwater for Sustainable Development*, vol. 14, Aug. 2021, Art. no. 100622, https://doi.org/10.1016/j.gsd.2021.100622.

[9] M. Mohapatra, S. Anand, B. K. Mishra, D. E. Giles, and P. Singh, "Review of fluoride removal from drinking water," *Journal of Environmental Management*, vol. 91, no. 1, pp. 67–77, Oct. 2009, https://doi.org/10.1016/j.jenvman.2009.08.015.

[10] T. Akafu, A. Chimdi, and K. Gomoro, "Removal of Fluoride from Drinking Water by Sorption Using Diatomite Modified with Aluminum Hydroxide," *Journal of Analytical Methods in Chemistry*, vol. 2019, Dec. 2019, Art. no. 4831926, https://doi.org/10.1155/2019/4831926.

[11] A. Amalraj and A. Pius, "Removal of fluoride from drinking water using aluminum hydroxide coated activated carbon prepared from bark of Morinda tinctoria," *Applied Water Science*, vol. 7, no. 6, pp. 2653–2665, Oct. 2017, https://doi.org/10.1007/s13201-016-0479-z.

[12] S. Ravulapalli and R. Kunta, "Defluoridation studies using active carbon derived from the barks of Ficus racemosa plant," *Journal of Fluorine*

Chemistry, vol. 193, pp. 58–66, Jan. 2017, https://doi.org/10.1016/j.jfluchem.2016.11.013.

[13] S. B. Ghosh and N. K. Mondal, "Application of Taguchi method for optimizing the process parameters for the removal of fluoride by Al-impregnated Eucalyptus bark ash," *Environmental Nanotechnology, Monitoring & Management*, vol. 11, May 2019, Art. no. 100206, https://doi.org/10.1016/j.enmm.2018.100206.

[14] A. Rastogi and S. K. Gupta, "Defluoridation Studies of Ground Water Using Natural Adsorbent Prepared From Mango Bark," *International Journal of Chemical & Petrochemical Technology*, vol. 8, no. 1, pp. 1–8, Jan. 2018, https://doi.org/10.24247/ijcptfeb20181.

[15] K. Shah, M. B. Patel, R. J. Patel, and P. K. Parmar, "Mangifera Indica (Mango)," *Pharmacognosy Review*, vol. 4, no. 7, pp. 42–48, 2010, https://doi.org/10.4103/0973-7847.65325.

[16] P. Scartezzini and E. Speroni, "Review on some plants of Indian traditional medicine with antioxidant activity," *Journal of Ethnopharmacology*, vol. 71, no. 1, pp. 23–43, Jul. 2000, https://doi.org/10.1016/S0378-8741(00)00213-0.

[17] V. Ganvir and K. Das, "Removal of fluoride from drinking water using aluminum hydroxide coated rice husk ash," *Journal of Hazardous Materials*, vol. 185, no. 2, pp. 1287–1294, Jan. 2011, https://doi.org/10.1016/j.jhazmat.2010.10.044.

[18] S. Ayoob, A. K. Gupta, P. B. Bhakat, and V. T. Bhat, "Investigations on the kinetics and mechanisms of sorptive removal of fluoride from water using alumina cement granules," *Chemical Engineering Journal*, vol. 140, no. 1, pp. 6–14, Jul. 2008, https://doi.org/10.1016/j.cej.2007.08.029.

[19] A. M. Raichur and M. Jyoti Basu, "Adsorption of fluoride onto mixed rare earth oxides," *Separation and Purification Technology*, vol. 24, no. 1, pp. 121–127, Jun. 2001, https://doi.org/10.1016/S1383-5866(00)00219-7.

[20] S. M. Maliyekkal, S. Shukla, L. Philip, and I. M. Nambi, "Enhanced fluoride removal from drinking water by magnesia-amended activated alumina granules," *Chemical Engineering Journal*, vol. 140, no. 1, pp. 183–192, Jul. 2008, https://doi.org/10.1016/j.cej.2007.09.049.

[21] N. Rajamohan, R. R. Kannan, and M. Rajasimman, "Kinetic Modeling and Effect of Process Parameters on Selenium Removal Using Strong Acid Resin," *Engineering, Technology & Applied Science Research*, vol. 6, no. 4, pp. 1045–1049, Aug. 2016, https://doi.org/10.48084/etasr.635.

[22] B. Nayak, A. Samant, R. Patel, and P. K. Misra, "Comprehensive Understanding of the Kinetics and Mechanism of Fluoride Removal over a Potent Nanocrystalline Hydroxyapatite Surface," *ACS Omega*, vol. 2, no. 11, pp. 8118–8128, Nov. 2017, https://doi.org/10.1021/acsomega.7b00370.

[23] S. Raghav and D. Kumar, "Adsorption Equilibrium, Kinetics, and Thermodynamic Studies of Fluoride Adsorbed by Tetrametallic Oxide Adsorbent," *Journal of Chemical & Engineering Data*, vol. 63, no. 5, pp. 1682–1697, May 2018, https://doi.org/10.1021/acs.jced.8b00024.

[24] A. O. Dada, A. P. Olalekan, A. M. Olatunya, and O. Dada, "Langmuir, Freundlich, Temkin and Dubinin–Radushkevich Isotherms Studies of Equilibrium Sorption of Zn 2+ Unto Phosphoric Acid Modified Rice Husk," *IOSR Journal of Applied Chemistry*, vol. 3, no. 1, pp. 38–45, 2012, https://doi.org/10.9790/5736-0313845.

[25] Y. S. Ho and G. McKay, "A Comparison of Chemisorption Kinetic Models Applied to Pollutant Removal on Various Sorbents," *Process Safety and Environmental Protection*, vol. 76, no. 4, pp. 332–340, Nov. 1998, https://doi.org/10.1205/095758298529696.

[26] J. C. Morris and W. J. Weber, "Removal of Biologically-Resistant Pollutants from Waste Waters by Adsorption," in *Advances in Water Pollution Research*, London, UK, Sep. 1962, pp. 231–266, https://doi.org/10.1016/B978-1-4832-8391-3.50032-4.